MV Discovery via Phasor Measurement Units

Maximiliano Pérez López, *Universidad Pontificia Comillas.*

***Abstract*— This thesis project studies PMU-based fault location in medium-voltage distribution networks with a focus on solutions that a utility could actually deploy. The core of the work aims to discover if a single-ended impedance estimator, supported by a small set of well-placed PMUs can deliver reliable locations without instrumenting the entire feeder. To keep costs realistic, PMUs are assumed at sites where previous monitors already exist. The choice is tied to quality of service, since quicker and more trustworthy location shortens isolation and restoration.**

A 43-node section of an urban Milan feeder serves as the case study. Faults are simulated across nine scenario families that combine three fault types with three fault-resistance levels of 0, 1, and 5 Ω. Phasors are extracted, apparent impedances are computed, and each PMU produces a location probability over the network. These per-sensor views are then combined through a Bayesian rule under a uniform prior. Performance is reported using correct-classification rate, posterior probabilities, and distance error both in metres and as a share of feeder length. For context, a baseline using only the head-end sensor is evaluated alongside the fused method.

The method resulted in three main findings. At low resistance the method performs strongly, in several 0 Ω cases it identifies 41 of 43 events, and the associated posteriors are high. As resistance increases, confidence and hit rate decline, which accords with established accounts of one-ended impedance methods, where the additional voltage drop across the fault is read as extra line length. Even so, the 5 Ω group shows average spatial errors that remain local, roughly 3.2 percent of feeder extent, keeping switching and patrol efforts near the true section. Against the single-sensor baseline, correct classifications fall by about a quarter at 0 and 1 Ω, and distance errors rise slightly. The results suggest a credible path for DSOs: incremental PMU deployment at legacy sites, a transparent impedance estimator, and probability-based fusion.

***Index Terms*— Phasor measurement units, fault location, distribution networks, MATLAB.**

I. INTRODUCTION

THE first electric power system (EPS) was developed in 1882 by Thomas A. Edison. It was a direct current (DC) system with the purpose of supplying energy to a small portion of the area of Manhattan in New York City [1]. Over the next 143 years that followed, EPSs have become an irreplaceable aspect of modern societies. Many, if not all, of our day-to-day activities are currently powered by electricity; offices, houses, hospitals, transport, they all depend on the supply of electrical energy to keep their function. Consequently, this has placed a great responsibility on the electrical industry to deliver safe, clean, and cheap energy to the rest of the industries. This involves the crucial concept of quality of service (QOS).

Due to the elevated dependency on electrical energy, cities and countries have increased their need for a continuous energy supply, and the constant reduction of interruption times. This is part of what is considered QOS, which focuses on guaranteeing the overall quality of the energy delivered from the power systems to the final customers, as well as the energy transfer between different sections of the grid.

One of the main causes of service interruptions in electrical networks are faults. Faults have many potential origins, from weather conditions, equipment malfunction, or even human error, faults negatively affect the grid's stability. Therefore, when a fault occurs, it is crucial to locate it as quickly and as accurately as possible, as the time taken to find and isolate the affected section will determine how long customers remain with interrupted supply. This turns fault location into an essential process for protection systems in EPS.

There are several traditional fault location methods, some of them still widely used, but they will face limitations when applied to modern grids. Traditional methods' accuracy may decrease as the grid becomes more complex, and the penetration of distributed generation keeps increasing. In the past years, this has led to the development of more advanced fault location techniques that can better adapt to current power system conditions. Among these, Phasor Measurement Units (PMUs) have gained much attention.

PMUs are able to provide time-synchronised measurements of voltage and current phasors from different points in the network. This allows operators to analyse faults with a higher level of precision, as the measurements from separate locations can be compared directly. PMU technology can be used along with traditional impedance-based fault location algorithms, which could reduce the uncertainty of the estimated location and facilitate the distribution system operators (DSOs) job at reestablishing power.

However, deploying PMUs across a distribution network can be a costly modernisation. Therefore, DSOs may be interested in strategies that reduce installation and maintenance costs without losing their benefits. Here is where a new approach is needed, to install PMUs in the same positions where existing measurement devices are already present, avoiding the need for additional infrastructure.

This project follows this approach and applies it to a section of a medium-voltage distribution grid located in Milan, Italy. The method combines a more traditional impedance-based fault location with a probabilistic refinement process that merges different location predictions into a single result. This is done using Bayes' Theorem, which allows the results from different PMU perspectives to be weighted and combined according to their likelihood. The performance of this method is evaluated by simulating different types of faults and fault resistances, comparing the intended result and the actual estimation.

II. Current Applications of PMUs in HV Transmission Networks

There is a large volume of published studies describing the role of PMUs in high voltage (HV) transmission networks. An increasing amount of literature is being published on the use of these devices for many applications such as fault detection and location, distance protection, stability, and Wide Area Monitoring System (WAMS). Recent developments in the field of power systems have led to a renewed interest in PMU-based protection schemes. The general consensus in the literature is that they improve stability, reliability, and efficiency.

Monitoring and Control

PMUs can provide precise and synchronised measurements, useful for advanced control strategies, grid automation, and system optimization. Thanks to this, PMUs contribute significantly to real-time monitoring of power systems. They offer Transmission System Operators (TSOs) detailed measurements of voltage and current phasors, which are crucial for identifying disturbances and assessing the overall health of the power system [3].

System Stability and Efficiency

PMUs are vital for enhancing system stability and operational efficiency in smart grids. Their measurements help in state estimation and voltage stability assessment [3].

Fault Detection

PMU technology has become instrumental in fault detection within the power grid. The microsecond accuracy allows for precise detection of disturbances like frequency variations and voltage instabilities.

The growth in the adoption of PMUs reflects their important role in improving the monitoring and control mechanisms of power grid operations, providing the accuracy and reliability necessary for modern grid management [3].

PMUs are used for wide-area fault detection and location, employing analytical methods that utilize dispersed synchrophasor measurements and bus impedance matrices to detect fault inception. This allows for the determination of the faulted zone, diagnosis of the suspected faulted line, and identification of the exact fault point along the line.

They can also detect multiple faults across a wide area network using signal processing approaches, where PMUs installed at various buses acquire synchronised voltage phasors [4].

These applications are all extremely useful for transmission line protection schemes, as well as monitoring. However, the focus of this study is fault location, so the document will gravitate towards that.

Fault location is a crucial area of research for EPS. Data extracted using PMU device has proven to be useful for improving traditional fault location methods, as well as opening the way for new, innovative approaches.

Fault Location Methods in Transmission Networks

IEEE Standard C37.114-2004 [5] mentions two different types of fault location methods. The first method, based on the estimation of line impedances, is often called in the literature as impedance-based. Impedances are commonly obtained using the equations developed and published by J.R. Carson, *et al*. in 1926 [6]. Naturally, the accuracy of this method depends on the accuracy of the impedance estimation method, which is high for Carson's equations.

A second method, often referred to as traveling wave, is defined by IEEE as "The resulting wave when the electric variation in a circuit takes the form of translation of energy along a conductor, such energy being always equally divided between current and potential forms" [6].

Impedance-based methods can be divided into two main categories: one-ended, known as single-ended, and two-terminal, also referred to as double-ended. These methods are explained below.

Single-ended

Single-ended, or one-ended, fault location techniques are widely used in transmission and distribution systems to estimate the location of faults using electrical measurements obtained exclusively from one terminal of the line. These methods are typically embedded in microprocessor-based protective relays and require specific equipment and data inputs to operate effectively.

The fundamental idea behind single-ended fault location techniques lies in estimating the apparent impedance seen from a single measurement point into the transmission line. This estimated impedance is then used to infer the distance to the fault. In order to obtain accurate results, it is generally necessary to measure phase-to-ground voltages and the corresponding phase currents across the three phases. However, phase-to-phase faults remain detectable even if only line-to-line voltage data is available. Furthermore, if the zero-sequence source impedance is known, estimates of phase-to-ground faults can also be obtained.

One of the simplest implementations of this approach is known as the reactance method. In this case, the fault distance is assumed to be proportional to the ratio between the measured reactance and the total line reactance.

Double-ended

Double-ended, or two-terminal, fault location methods utilize data collected from both ends of a transmission line to determine the location of the fault. These methods are generally more accurate than one-ended techniques due to their ability to mitigate common sources of error.

Unlike single-ended methods that rely solely on local measurements, double-ended methods use voltage and current data from both ends of the line. This comprehensive data allows for more accurate calculations. One of the main advantages of these methods is their ability to minimize the negative effects of variations such as fault resistance and load current in their predictions, which are one of the major sources of error in single-ended methods.

One of the main disadvantages of double-ended methods is, naturally, their need to gather data from both ends and then process it at a single location. This characteristic turns the data acquisition and processing into much more complex stages than those in single-ended methods. Another important disadvantage is their speed. These location techniques generally require more time to generate an estimate, and although speed may not be critical for some applications, a longer location estimation time can lead to longer downtime and interruptions, negatively impacting the grid's QOS.

PMUs in MV Distribution Networks

Applications

In a review published by Menezes et al. [4], the authors mention different applications related to distribution systems, they particularly highlight fault detection and location, state estimation, islanding detection, and other protection schemes.

The papers reviewed are significantly fewer than those related to transmission applications. From a total of 39 research papers proposing new approaches to PMU integration in EPS, a total of 32 were focused on transmission systems, while only 8 researched distribution-level areas, with 4 of them being microgrids. However, 2 of those papers focus on general protection. That means only 1 paper from the 39 reviewed is truly relevant to fault location.

In the research paper published by Pignati et al. [12], it is claimed that PMU-based protection schemes possess the needed characteristics required for time-critical situations such as fault location.

III. Challenges of PMU Implementation in MV Networks

An important aspect to consider is the challenges that come with working in medium-voltage (MV) distribution networks. While PMUs have been extensively developed and integrated to operate in HV transmission networks, the challenges that distribution presents are not equivalent to those of transmission. This means that the particular limitations related to MV grids will have to be considered to adapt PMU technology to these new applications.

Installation and Maintenance Costs

Despite their attractive advantages, PMU deployment carries several challenges that need to be considered. One of these challenges is the costs related to installation and maintenance activities. Considering general PMU implementation costs, that is, both transmission and distribution levels.

The U.S. Department of Energy offers a brief sight of the related costs concerning these deployments in [13]. This document sheds some light on the average investment required by these devices. It shows a median of 43,400 USD per PMU installed. This value includes the cost of each device as well as every installation-related cost such as design, labour, materials, and construction.

Economies of scale do not benefit this particular type of devices. That means that there is no cost decrease associated with the large-scale PMU deployment.

Nevertheless, it is important to note that the results shown in these reports vary in magnitude (i.e. some projects presented costs double or half the median cost) [13].

However, research suggests that it is possible that through optimal PMU placement, high costs and communication infrastructure issues might be reduced. In reference [14], Cruz et al. propose an optimization algorithm for centralised WAMS. This paper presented an optimization algorithm that managed to reduce PMU installation costs for certain applications. This proposal was tested in various IEEE test networks, including a practical application in a 5804-bus Brazilian transmission system. The results demonstrated flexibility and effectiveness, with a promising scalability and adaptability. These results contradict the conclusions presented in the recovery Act from the U.S. government.

IV. Justification

As modern power systems evolve to accommodate high levels of distributed energy resources (DERs), electric vehicles, and bidirectional energy flows, medium voltage (MV) distribution networks face increased complexity. Fault detection and location are now more challenging than ever, yet critical for protection schemes, focused on maintaining reliability and minimising downtime. Phasor Measurement Units (PMUs) offer an attractive solution by providing time-synchronised measurements. However, their adoption in MV networks has been hindered by high costs, complex installation requirements, and the traditionally dense deployment needed for effective coverage.

Research has shown that DER penetration has a negative impact in the stability and reliability of distribution networks. In a study done in 2022, M. S. Turiman *et al*. analysed and studied the technical impacts that distributed generation (DG) had in distribution grids. The consensus was that one of the main effects of DG integration was an increase in fault level, especially related to synchronous and asynchronous machines. Other findings were that DG integration had the potential to affect voltage regulation, cause voltage limit violation, increased network losses, and increased line loading [17].

However, DER not only have negative impacts, Ref. [18] studied the impact of Battery Energy Storage Systems (BESS) on distribution networks. In this paper, the authors found that BESS had a positive impact on the grid in which they were implemented. They appeared to improve stabilization by facilitating a fast response, as well as reducing the negative effects of disturbances and improving the power quality of the grid.

It is also important to note that while a low presence of DG in the grid is normally manageable, when that presence reaches a percentage higher than 20%, outages start to become much more likely and critical. Ref. [19] highlights how much DG impacts distribution networks.

This project addresses these shortcomings by developing and testing a PMU-based fault location method for MV networks that provides higher-quality data. The methodology is built around realistic data and conditions: it utilises real measurements provided by Gridspertise, along with a MATLAB Simulink simulation that accurately models the behaviour of MV distribution grids under fault conditions.

The method centres on single-ended, impedance-based fault location algorithms, chosen for their low infrastructure requirements and compatibility with existing utility devices. However, unlike traditional single-ended methods, the approach proposed in this project introduces enhancements aimed at maximising the value of each PMU by using a tailored measurement placement strategy and adapted fault analysis to compensate for the reduced observability.

The value of the proposition is clear, to use fewer PMUs to achieve accurate fault location. This can significantly reduce capital and installation costs. Faster and more efficient fault detection will minimise outage times and improve service reliability indicators like System Average Interruption Duration Index (SAIDI) and System Average Interruption Frequency Index (SAIFI). Deployment is more realistic and scalable, as the system can operate effectively even in partially monitored networks.

Using real PMU data from an industry partner improves the applicability of the approach, while the simulation testing allows for a flexible analysis of performance under diverse scenarios and fault types without the technical and economic complications of real grid testing.

This project aims to offer a commercially and operationally viable alternative to populate networks with PMU technology by balancing performance and practicality. It gives utilities a path to benefit from the protection and monitoring capabilities of PMUs without the financial and technical burden of making entirely new installations. The proposed method aligns with the goals of smart grid modernisation, especially in regions where investment in new infrastructure must be carefully analysed.

In conclusion, this project aims to deliver a cost-effective solution for PMU-based fault location in MV distribution systems. It combines academic content with industrial relevance, building a bridge between research and deployment. For distribution system operators (DSOs), the result is a method that provides the benefits of synchrophasor data while optimizing economic investment and reducing the need for large-scale infrastructure deployment.

V. Model & Algorithm Developed

MV Distribution Grid

The case study selected for the development of this project corresponds to a 43-node MV distribution network, which forms part of a larger and more complex grid located in the city of Milan, Italy. Rather than implementing and testing the proposed methodology across the entire distribution system, which would have posed significant challenges in terms of complexity, computational requirements, and result interpretation, as well as time investment, a decision was made to focus the study on a smaller subsection of the grid.

This decision allowed for a more controlled and efficient evaluation of the algorithm's performance. The selected section includes 43 nodes, distributed across several radial branches and its respective amount of topological characteristics characteristic of typical urban MV networks. This portion of the grid is depicted in Figure 1.

In order to simulate the grid and apply the fault location algorithm effectively, a number of assumptions were introduced. These assumptions helped define and limit various aspects of the project, from the structure and configuration of the simulation model to the implementation and limitations of the algorithm. The most relevant assumptions are briefly described below:

As discussed earlier, to reduce infrastructure and installation costs, PMUs are assumed to be installed in the same physical locations where previous measurement devices, which in this case study are RGDMs, were deployed. This strategy is critical to the project's cost-efficiency goal, as it uses existing infrastructure to avoid the need for significant additional investment, turning this proposal into a much more attractive option.

Currently, due to technological limitations, it remains infeasible to obtain PMU-grade measurements directly from the header of the grid. As a result, data obtained from the header do not reflect the same level of time-synchronised accuracy as those obtained from the PMUs installed at the rest of the nodes. While this introduces a degree of uncertainty into the dataset, it represents no critical disadvantage as its impact is mitigated by the combination carried by the algorithm.

To address the limitations introduced by the absence of a PMU at the grid header, the algorithm relies on data gathered from multiple PMUs strategically distributed throughout the network. In this specific case, five PMUs were deployed at critical locations, all of them with both remote control and RGDM sensors present beforehand. This allows the algorithm to obtain more information that then translates into a more accurate prediction method. This proposal improves the robustness of fault location predictions and compensates for any inaccuracies potentially introduced by non-PMU data sources.

The core principle behind the algorithm is the estimation of the fault distance by comparing the expected, pre-fault, line impedances with the actual impedances measured during a fault event. By doing so, the algorithm is able to calculate a set of possible distances for each observation point. These estimated distances are then combined, and their consistency evaluated, to produce a final prediction of the fault location along with an associated likelihood or confidence level.

RTDS Model

To properly test the algorithm, the first step is to create a model the respective grid in a simulation software. This modelling process was conducted at the laboratories of Gridspertise in Milan, Italy, with technical support from the company. And then adapted specifically for the purposes of this study.

The model was modified to include a configurable fault component, allowing the faults to be activated at any of the 43 nodes in the network. Additionally, controllable switches were integrated to selectively activate or deactivate specific fault types. Then the resulting voltage, current, and frequency values were captured by all 5 PMU sensors and stored in folders within the software in real-time. This way, the fault location could be chosen at any point and changed whenever needed.

PMU devices were placed in their corresponding locations, header and nodes 10, 20, 26, 30. This distribution covers the entire grid and guarantees a proper observability of the grid.

The core idea was to use the model in the RTDS software to simulate in real-time the faults that were to be analysed in this study. The study focused on 9 different scenarios, which encompass 3 different fault types and 3 fault resistance values, stated as follows.

The fault types under analysis were:

- 3-Phase
- Double-line-to-ground
- Line-to-line

Similarly, these 3 fault types were simulated in 3 different fault resistance conditions, i.e., three different FR values:

- FR= 0Ω
- FR= 1Ω
- FR= 5Ω

As each one of the three fault conditions is analysed under other three FR conditions, the results amount to nine unique simulations with individual results.

To achieve this, the model had to be simulated and automated to facilitate the extraction process. This was carried out through a script implemented in the RSCAD software that runs the RTDS simulation. This script handled the currently simulated fault location to switch from one FR value to the next, and then from one FT to the next. Each time the script finished obtaining the relevant voltage and current data, it then created a CSV file to store it and saved it in the proper folder within the device. This required the manual modification of the model to place the fault in each one of the 43 nodes within the grid.

Although the automation script streamlined much of the process, manual intervention was still required to reposition the fault component across all 43 nodes of the network, one by one. Once data had been generated for all nodes and fault scenarios, the resulting data folders were transferred to the computing environment where the main fault location (FL) algorithm was executed and evaluated.

MATLAB System

The system is implemented in MATLAB, utilising a central orchestration script that interacts with many specialised functional modules, including its main: a DFT module for waveform processing, an impedance calculation for impedance-based localisation, and a fault classifier that classifies the fault into one of 4 possible types.

The proposed system addresses the challenge of rapidly and accurately identifying fault locations by processing large volumes of simulated fault data from a Real-Time Digital Simulator (RTDS). The methodology is structured to first identify potential fault zones using individual PMU measurements (Stage 1) and then refine this localisation by probabilistically combining information from multiple PMUs (Stage 2). The main script manages the overall workflow, from data ingestion and organisation to the execution of the two analytical stages and the presentation of final fault location predictions.

Stage 1: Traditional Distance Protection

The first stage of the localization process makes use of conventional impedance-based principles to determine individual fault locations from the perspective of each individual PMU.

Waveform Phasor Extraction

For each PMU measurement associated with a given fault scenario, the script calls the DFT_v7.m model to apply the Discrete Fourier Transform to the respective waveform obtained from the CSV data. This takes the path to the raw waveform CSV file and the nominal system voltage (Vn) as inputs. Figure 1 shows the waveform signal in MATLAB.

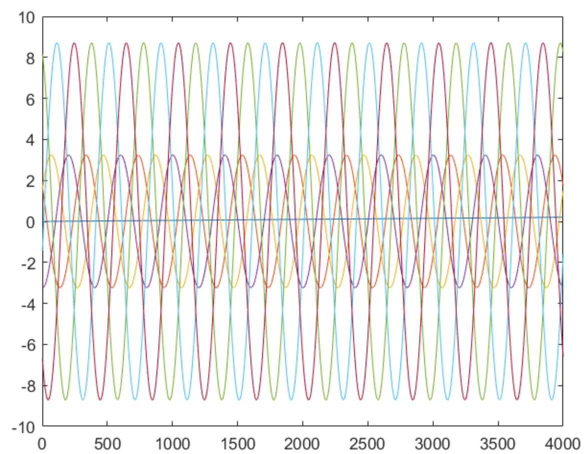

Figure 1. Waveform signal for the algorithm. Y axis: current (kA); X axis: time (s).

Within this module, the time-series voltage and current data are processed using the DFT. This function extracts the steady-state phasor components, including positive, negative, and zero sequence voltages (E1, E2, E3, E0a, Eda, Eia) and currents (I1, I2, I3, I0a, Ida, Iia). These phasor values serve as the fundamental electrical measurements for the fault analysis done in the rest of the process.

Impedance-Based Fault Zone Identification

This module receives the grid node ID corresponding to the measuring PMU, the pre-loaded grid and node topology data, HV system parameters, feeder details, nominal voltage, and the specific PMU's waveform file path.

Initially, the grid's impedance matrices (positive and zero sequence, Zd, Z0) are computed using the get_imped_matrix_v5 function, establishing the electrical characteristics of each line and node. This function calculates the baseline impedances as seen from each one of the buses in the grid. This is a critical step, as the distance calculation depends on the comparison of baseline impedances and apparent impedances. In Figure 2, the results of this identification are visible.

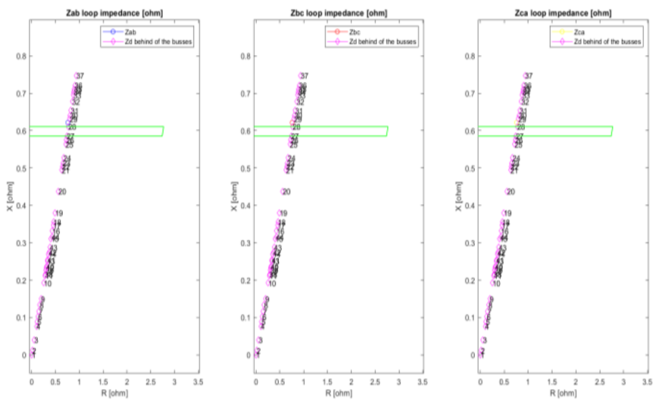

Figure 2. Impedance location.

However, the analysis results must consider the different fault types that the data might correspond to. With this in mind, a fault classifier sub-function is implemented to analyse the symmetrical components of the phasors during the fault period to determine the specific fault type (e.g., three-phase, line-to-line, or double line-to-ground). Once the fault type is calculated, there is another critical action that the script must tackle to ensure that the results are accurate.

Fault Type Filter

The script uses fault currents and voltages to calculate the apparent impedance and then makes a comparison between that and the baseline bus impedance. This information is then used to make a prediction of the fault location. However, PMUs do not always see a fault, as it may be located outside of their point of view. This may lead to false predictions as the algorithm must give a prediction regardless of the data. It is for this reason that a filter is implemented. Figure 3 shows a typical unfiltered current signal that is part of the signal inputs to the algorithm.
Based on the fault type detected by the fault type classifier, the filter sets a series of conditions that, if met by the fault data, will classify the prediction as a "no fault" prediction. This is done by analysing the current values and based on the fault type, setting a threshold that divides fault current levels from normal current levels. This means that the data sets detected with normal current levels will have their predictions set as "no fault seen", which provides useful information for the final prediction. The result is that if a PMU detects no fault, then the rest of the predictions have a higher value, as the fault is not present in this zone.

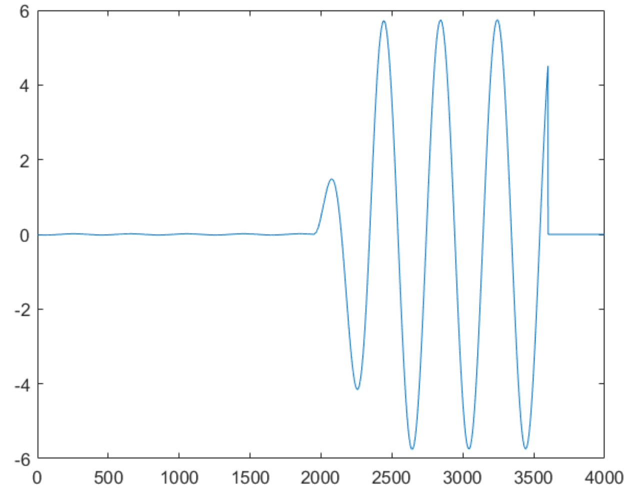

Figure 3. Unfiltered current signal. Y axis: current (kA); Y axis: time (s)

Results

After the data has been filtered, the apparent impedance observed at the PMU location is calculated. This apparent impedance is subsequently mapped onto predefined MHO relay characteristic zones associated with each node in the distribution network, utilizing the Z_map function. This mapping process quantifies the likelihood that the observed fault impedance falls within the protective zone of each node.
The primary output of this stage, for each individual PMU, is a percentage vector. This vector represents a probability distribution, indicating the percentage likelihood of the fault being located at each specific node in the system, purely based on the measurements from that single PMU. For numerical stability in the subsequent stage, a small smoothing factor (ϵ) is applied to these percentages, ensuring no zero probabilities, and the vector is normalized to sum to unity.

Stage 2: PMU Refinement

The second stage focuses on refining the predicted fault location results by combining the individual probabilities (likelihoods) obtained from multiple PMUs using Bayes' Theorem. This integration takes advantage of several PMU measurements to improve the prediction accuracy and reduce the ambiguity inherent in the individual measurements.

Bayesian Combination of Fault Location Probabilities

The proposed algorithm relies on PMU data to estimate the location of faults in a distribution network. Due to the nature of electrical faults and the distribution of PMUs across the system, each measurement point provides a partial and independent perspective of the event. These perspectives are expressed as probabilistic fault location estimates for each possible bus in the network. In order to reach a final, consolidated prediction of the faulted location, the algorithm uses a Bayesian combination method to integrate the multiple estimates into a single, coherent probability distribution.
The core idea is to treat the outputs from different PMU viewpoints as conditionally independent likelihoods of the fault being at each node. By assuming a uniform prior probability

(i.e. there is no prior knowledge for any specific node over another), the code applies Bayes' Theorem to update this prior probability using the available likelihoods.

Each iteration of the loop in the code corresponds to one group of six likelihood values (e.g., from six different PMU measurements) and for each of the 43 possible fault locations. The key steps of the algorithm are the following:

Prior Definition

A uniform prior probability distribution is assumed for all possible fault locations. Reflecting the temporary assumption that all nodes are equally likely to experience a fault.

Likelihood Aggregation

For each set of six probability columns, representing different views or methods of estimating the fault likelihood, the algorithm computes the product of the likelihoods for each location. This step combines the individual observations into a single combined likelihood for each node. This aligns with the assumption of conditional independence.

Posterior Calculation

Then, the unnormalized posterior values are computed by performing an element-wise multiplication of the prior and the combined likelihoods. This results in an intermediate vector that represents the relative belief that each node is the faulty node, before normalisation.

Normalization

To make sure that the final values represent a valid probability distribution (i.e. they sum to 100%), the unnormalized posterior is scaled accordingly. This results in the final Bayesian posterior probabilities, which are stored in a vector.

The algorithm aims to improve the robustness and reliability of the fault location prediction by combining all the different estimates through this probabilistic framework. Bayes' Theorem allows for the fusion of independent evidence, improving its accuracy, especially in cases where some measurements may be noisy, ambiguous, or do not provide enough information when interpreted in isolation. This happens especially often when the PMU is located before a branch separation that leads to 2 or more branches with one of them containing the fault. In these cases, the PMU calculates a distance that corresponds to several different nodes, which leads to multiple predictions with similar likelihoods.

VI. Results and Discussion

As mentioned in the previous chapter, the algorithm begins the process by extracting the fault data from the CSV file that contains the measurements recorded during the fault event. Then, this information is presented in the form of waveforms to facilitate their processing. This waveform is also plotted in an effort to facilitate the visualisation of the fault behaviour, which in turn aids troubleshooting as well. The rest of the algorithm will use the voltage and current phasors in their rectangular form, $a + ib$. These values are the core of the calculations and are used throughout the entire process to calculate the impedances that will bring the results.

After reading and adapting the data, the impedance estimation stage will produce several outputs. These include the following.

Location estimates provided by each PMU individually

The likelihood distribution for each of the estimates

A graph visually showcasing the comparison between the measured impedance (during the fault event) and the baseline bus values

The voltage and current waveforms associated with the fault.

In this case study, the system includes five PMUs and one non-PMU sensor located at the header of the grid. Together, they provide a total of six separate fault location estimates. Then, in order to obtain a single final prediction, these individual estimates are combined using Bayes' Theorem. This combination step produces two outputs.

- A Bayesian combined estimate
- Probability values for each possible fault location.

It is important to note that some of the individual estimates may be, and surely will be, incorrect. This results in estimations that differ from the actual faulty node. To consider this and allow for analysis, the distance between the estimated and the actual faulty node is calculated by computing the difference between the predicted location and the true location once the algorithm shows its results. This metric helps build a more detailed assessment of the accuracy and reliability of the proposed method.

The proposed Bayesian fusion approach was tested on a 43-node urban feeder model under nine scenario families, combining three fault types (single-phase-to-ground, double-phase, and three-phase) with three fault resistances (0, 1, and 5 Ω). Performance was assessed in terms of correct-classification rate, posterior probability, and distance error, and benchmarked against a baseline method that relies solely on the feeder head PMU.

For low-resistance faults ($R_f = 0$ Ω), the method achieved high accuracy. In several three-phase cases, the algorithm correctly identified 41 out of 43 events, with posterior probabilities exceeding 99.95%. Distance errors were negligible, confirming that the single-ended impedance estimator performs reliably when additional fault resistance does not distort apparent impedance.

At $R_f = 1$ Ω, a moderate decline in performance was observed. Classification rates dropped by approximately 15–20%, and posterior probabilities decreased accordingly. These results are consistent with theoretical expectations, as the added resistance introduces a voltage drop that biases the estimator toward longer apparent line lengths. Nonetheless, distance errors remained moderate, and the Bayesian combination helped preserve robustness by down-weighting inconsistent estimations.

The most challenging case was $R_f = 5$ Ω, where accuracy declined further, and several events were misclassified. However, the spatial analysis showed that the average error remained limited to about 266.9 m, corresponding to roughly 3.2% of the feeder length. Thus, while classification accuracy diminished, fault localization still remained sufficiently close to the true section to be operationally useful.

A comparison with the single-sensor baseline underscores the value of Bayesian fusion. Using only the head-end PMU reduced correct-classification rates by about 20–25% in the 0 and 1 Ω scenarios and produced slightly larger distance errors. This confirms that combining multiple measurement perspectives significantly improves accuracy and mitigates local biases associated with single-point estimation.

Overall, the results demonstrate that the proposed approach maintains high accuracy at low fault resistance, degrades in a controlled manner as resistance increases, and consistently outperforms a single-sensor benchmark.

DISCUSSION

Once all results are considered together, the pattern becomes easier to see. Figure 4 presents the average estimation probability for the three fault types across the three-fault resistance (FR) levels. A consistent tendency appears, as FR increases, the mean estimation probability tends to drop. This behaviour was expected and is visible in the figure for all three

Figure 4. Average Estimation Probability (%)

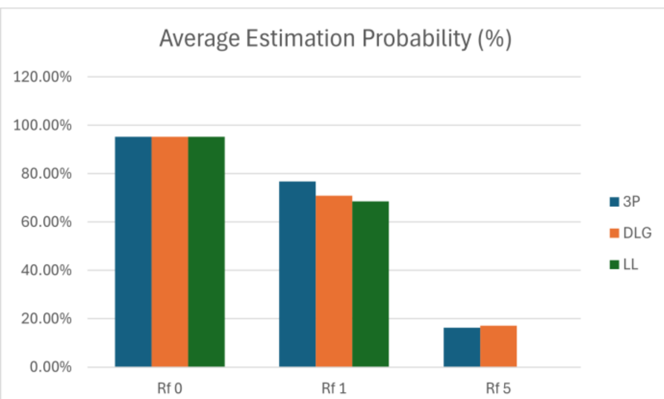

fault categories, where the estimation values decline as the FR moves from 0Ω to 1Ω to 5Ω.

Estimation probability alone, however, does not fully describe the method's behaviour. A second viewpoint is needed for this. Figure 5 reports the percentage of correct estimations for each scenario in the analysed grid. The numbers closely track those in the previous figure, which is reasonable because most correct classifications carry probabilities very close to 100 percent. As a result, the average probability and the share of correct outcomes move in parallel.

It is also clear that the predictions obtained with an FR of 5Ω show lower probabilities and reduced accuracy. Yet this count of correct cases relies on a binary decision: either the estimate matches the true node, or it does not. To better interpret the results, it is necessary to add a measure that reflects how far a wrong estimate is from the actual faulted section.

Figure 6 offers that perspective by plotting the distance between the node predicted by the algorithm and the true location. This view helps to judge the severity of errors rather than only their occurrence. The pattern is straightforward, low FR values lead to small distances. More interestingly, the 5Ω scenarios still produce an average spatial error of about 3.2 % of the grid's extent, which is not especially large. This reframes the earlier accuracy figures and provides a more balanced view of performance under higher resistance.

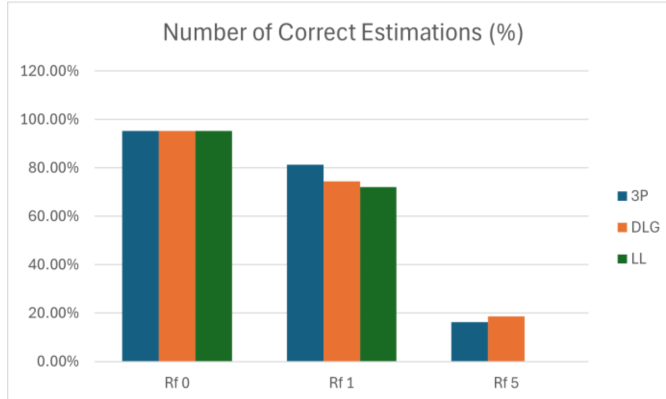

Figure 5. Number of Correct Estimations (%)

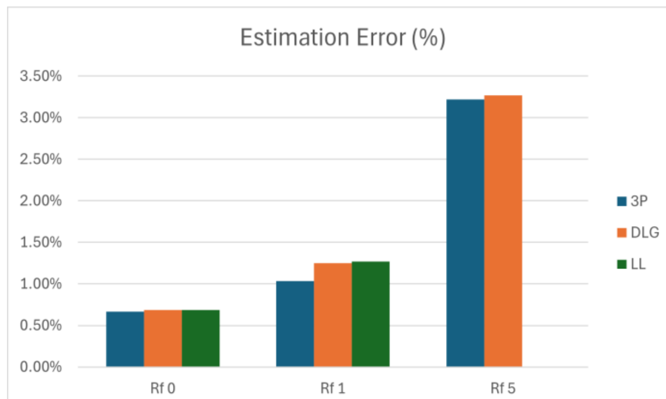

Figure 6. Estimation Error Distance (%)

The reason for the degradation at 5Ω is consistent with the theory of single-ended, impedance-based location. The additional voltage drop across the fault resistance is interpreted as part of the line, so the apparent impedance becomes the sum of the true line segment and a term that scales with FR and the fault type. If the model is tuned around lower FR, that extra drop is read as extra distance, creating a bias that grows with resistance. A higher FR also lowers fault current, reducing the contrast between pre-fault and fault phasors; residual load components, infeed, and modest measurement errors therefore matter more. For ground faults, zero-sequence paths and grounding impedances can further disturb simplified positive-sequence assumptions and add to the error.

Even so, the 5Ω simulations in this study do not show extreme deviations. Three factors likely explain this outcome.

First, the phasors are clean, and parameters are well specified, which reduces noise that would otherwise magnify high-resistance effects. Third, the approach combines viewpoints from multiple PMUs, this means that weaker estimates lose weight when results are fused, and the final location tends to be pulled toward the more reliable predictions.

Taken together, these observations suggest that FR is more impactful in performance than fault type. In practical terms, the method behaves consistently across the three fault categories as long as the resistance level remains comparable.

Comparison vs. Baseline Case

All these results are interesting on their own, but the value of the obtained outcomes does not only rely on their isolated values, but also on their performance when compared to other methods' results. In an effort to further visualise these methods' accuracy, the obtained data is compared to a baseline in this section.

The algorithm computes its estimations based on the data obtained from each one of the measurement points in the grid and then combines six different estimation data sets to end up with only one set of estimation data. This baseline case relies on a single measurement point at the head of the grid and instead of combining the resulting predictions with others, it estimates based solely on that one set of information. Naturally, this will mean that the amount of information with which the algorithm uses to produce a prediction is less than this study's case, and thus it is expected to have a lower accuracy and higher error ratio.

When set against the Bayesian combination, it can be seen that the baseline accuracy is smaller, the correct classification rate decreases by about 23.26% in FR 0Ω and 1Ω scenarios, from 95.35% to 72.09% for 0Ω and from 81.40% to 58.14% for 1Ω, while the third FR scenario presents only a small difference in value. This is all visible in Figure 7.

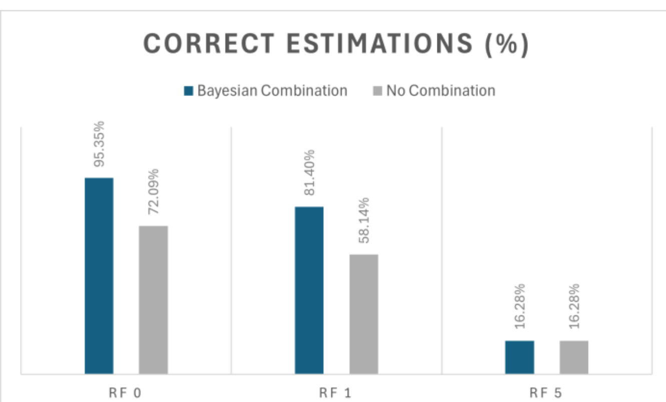

Figure 7. Percentage of Correct Estimations.

Several factors are likely to contribute to this gap. Firstly, a head-end point of view offers limited visibility of deep feeder sections, as the fault lies farther from the substation, the distinctiveness of the measured phasors is decreased. Also, with higher fault resistances, the extra voltage drop across the fault is read by the estimator as additional line length, which biases the apparent impedance even further, which is visible in Figure 8.

From an operational perspective, the differences are modest but not trivial. A reduction in correct identifications implies more switching steps or extra field checks before location, while the added distance error translates into longer patrol distance. Where the infrastructure supports multiple PMUs, the Bayesian fusion is preferable. If only a head-end PMU is available, the baseline still offers a somewhat decent performance, but its limitations should be expected to increase in high-resistance scenarios. Future work could examine whether lightweight compensation for fault resistance, or adaptive reweighting of PMUs based on past performance, narrows the remaining gap without adding significant complexity.

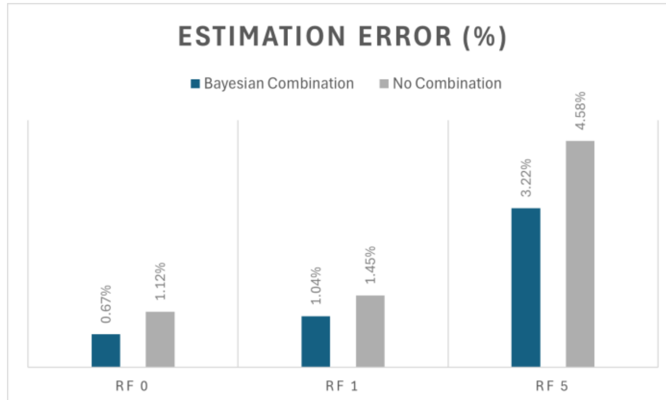

Figure 8. Distance to Actual Fault (%).

The Bayesian combination of different probabilities proves useful to increase the certainty of a fault being in a certain location. Each individual measurement point, whether it is PMU or not, is capable of delivering a limited certainty that a fault is located in any given portion of the grid. The Bayesian consideration of previous probability helps this "current probability" increase with any extra information that can be extracted from the scenario and ultimately increases the overall probability and therefore, the accuracy of this method.

In this study, the Bayesian comparison yields a 32.25% improvement in estimation capability for FR 0 scenarios and a 32.98% improvement for FR 1 scenarios. Taken together with the distance results, these gains support the use of multi-point fusion for location in the analysed grid, while also indicating where further refinement should focus.

VII. Conclusions and Future Work

This project set out to improve fault location in medium-voltage distribution networks while keeping deployment costs realistic. The method combines a single-ended impedance estimator with a Bayesian step that combines several perspectives, prioritising PMU placements that coincide with existing measurement sites to limit new infrastructure. The broader motivation of the study is quality of service (QOS), a faster and more reliable location shortens isolation and restoration, which supports continuity for customers and safer operations.

Methodologically, the work proceeds along two tracks. First, it builds a reproducible pipeline that ingests event waveforms, forms phasors, computes apparent impedances, and maps these to likely positions along the feeder. Second, it merges per-sensor outputs into a single posterior using Bayes' theorem with simple priors. The case study is a 43-node urban feeder in Milan, chosen to keep analysis tractable while retaining realistic features such as branching laterals and varied sequence parameters. PMUs are assumed at legacy monitor sites so the study can ask not only whether accuracy improves, but whether the gains arise in a way a DSO could plausibly adopt.

Across nine scenario families that cross three fault types with three resistance levels, three patterns emerge. At low fault resistance the method performs well, in several 0 Ω cases correctly identifying most events with high posterior probabilities. As resistance increases, accuracy declines, which aligns with single-ended impedance theory because the extra drop across the fault is interpreted as additional line length. Even so, at 5 Ω the distance errors remain moderate: the average error is close to three per cent of the grid's extent, which keeps switching and patrol effort local rather than feeder-wide.

In this case, the distance matters because a simple judgement whether its estimation is correct or not does not convey how far a wrong estimate lies from the true section. The distance metric contextualizes these results. Low resistances cause small deviations, and a higher resistance, while it lowers the number of correct estimations, still produces errors that cluster near the correct area. This means that even though higher resistance levels may cause the estimations to be incorrect, estimated locations do not fall far away from the faulty section. With this, it can be expected that this method degrades in a controlled manner under added resistance, which is precisely the condition that often complicates field work.

To reinforce this analysis, a structured comparison with a single-sensor baseline is carried out. Relying only on the head-end viewpoint reduces observability of deeper feeder sections. In the results, correct classifications fall by roughly 32% in the 0 Ω and 1 Ω groups, and distance errors rise slightly. This is consistent with local bias from branching, infeed, and resistance-induced drops that the single point reads as extra length. Fusion reduces the impact of these effects by reducing weak perspectives and concentrating probability on candidates supported by multiple sensors.

Additionally, the deployment implications are considered. Reusing existing sites is a pragmatic compromise between ideal placement and cost. This decision facilitates implementation and eases smart grid modernisation.

However, the algorithm presents a key limitation. The header measurement device has weaker synchronisation than PMU-grade points, which is detrimental to the results when that perspective dominates. PMU installation on the header of the grid is not yet technologically feasible, which limits options to counter this problem. Even then, the potential affected estimations would be located closer to the header, which helps mitigate any inaccuracies.

Even with its limitation, the possible applications are clear. For operators, multi-PMU fusion offers clear improvement over a single sensor, particularly for distant faults and non-negligible resistance. The distance-based view suggests that a small set of well-placed PMUs can shorten patrol lengths and reduce the number of switching steps before isolation. For planners, the results point to incremental deployment tied to legacy sites, and to treating resistance compensation and calibration as first-order concerns.

The work also identifies concrete next steps. Modest fault-resistance compensation inside the estimator, tuned to local parameters, could reduce bias that grows with resistance. Relaxing the independence assumption during fusion, through covariance-aware weighting or learning sensor reliability from past events, may help. Testing resilience under noise, dropouts, and timestamp jitter, together with ablations that remove individual PMUs to measure marginal value, would further clarify applicability.

In summary, a single-ended impedance method, paired with simple probabilistic fusion across a handful of strategically located sensors, can provide accurate and operationally useful fault locations on an urban MV feeder. Although performance falls with increasing resistance, spatial errors remain contained, and fusion outperforms a single head-end baseline by a meaningful margin. The combination of practical placement, transparent computation, and clear reporting offers a credible path from study to deployment, and a foundation for incremental refinements that target the most consequential sources of error.

VIII. References

[1] D. and I. S. Banerjee Binayak and Jayaweera, "Fundamentals of Power Systems," in Smart Power Systems and Renewable Energy System Integration, D. Jayaweera, Ed., Cham: Springer International Publishing, 2016, pp. 1–13. doi: 10.1007/978-3-319-30427-4_1.

[2] A. G. Phadke, M. Ibrahim and T. Hlibka, "Fundamental basis for distance relaying with symmetrical components," in IEEE Transactions on Power Apparatus and Systems, vol. 96, no. 2, pp. 635-646, March 1977, doi: 10.1109/T-PAS.1977.32375.

[3] S. S. Yu, Md. S. Rahman, G. Zhang, S. T. Meraj, and H. Trinh, "Comprehensive review of PMU applications in smart grid: Enhancing grid reliability and efficiency," Chinese Journal of Electrical Engineering, pp. 1–41, 2025, doi: 10.23919/CJEE.2025.000129.

[4] T. S. Menezes, P. H. A. Barra, F. A. S. Dizioli, V. A. Lacerda, R. A. S. Fernandes, and D. v. Coury, "A Survey on the Application of Phasor Measurement Units to the Protection of Transmission and Smart Distribution Systems," Electric Power Components and Systems, vol. 52, no. 8, pp. 1379–1396, 2024, doi: 10.1080/15325008.2023.2240320.

[5] "IEEE Guide for Determining Fault Location on AC Transmission and Distribution Lines," in IEEE Std C37.114-2004, vol., no., pp.1-44, 8 June 2005, doi: 10.1109/IEEESTD.2005.96207.

[6] J. R. Carson, "Wave propagation in overhead wires with ground return," The Bell System Technical Journal, vol. 5, no. 4, pp. 539–554, 1926, doi: 10.1002/j.1538-7305.1926.tb00122.x.

[7] S. Marx, B. P. Administration, B. K. Johnson, A. Guzmán, V. Skendzic, and M. v Mynam, "Traveling Wave Fault Location in Protective Relays: Design, Testing, and Results."

[8] S. Das, S. Santoso, A. Gaikwad, and M. Patel, "Impedance-based fault location in transmission networks: Theory and application,"

IEEE Access, vol. 2, pp. 537–557, 2014, doi: 10.1109/ACCESS.2014.2323353.

[9] H. Mirshekali, R. Dashti and H. R. Shaker, "A Novel Fault Location Algorithm for Electrical Networks Considering Distributed Line Model and Distributed Generation Resources," 2020 IEEE PES Innovative Smart Grid Technologies Europe (ISGT-Europe), The Hague, Netherlands, 2020, pp. 16-20, doi: 10.1109/ISGT-Europe47291.2020.9248755.

[10] K. Zhuang, S. Mou, H. Chen, M. Cui, and L. Wang, "A Fault Location Method for Modern Distribution Network Based on Fault State Estimation by Hybrid Measurement," in 2024 8th International Conference on Smart Grid and Smart Cities, ICSGSC 2024, Institute of Electrical and Electronics Engineers Inc., 2024, pp. 141–146. doi: 10.1109/ICSGSC62639.2024.10813844.

[11] H. Mirshekali, R. Dashti, A. Keshavarz, and H. R. Shaker, "Machine Learning-Based Fault Location for Smart Distribution Networks Equipped with Micro-PMU," Sensors, vol. 22, no. 3, Feb. 2022, doi: 10.3390/s22030945.

[12] A. Pal, A. K. S. Vullikanti and S. S. Ravi, "A PMU Placement Scheme Considering Realistic Costs and Modern Trends in Relaying," in IEEE Transactions on Power Systems, vol. 32, no. 1, pp. 552-561, Jan. 2017, doi: 10.1109/TPWRS.2016.2551320.

[13] U.S. Department of Energy, Electricity Delivery and Reliability, "Synchrophasor technologies and their deployment in the recovery act smart grid programs," Aug. 2013. [Online]. Available: http://energy.gov/sites/prod/files/2013/08/f2/SynchrophasorRptAug2013.pdf

[14] Cruz, Marco & Rocha, Helder & Paiva, Marcia & Segatto, Marcelo & Camby, Eglantine & Caporossi, Gilles. (2019). An algorithm for cost optimization of PMU and communication infrastructure in WAMS. International Journal of Electrical Power & Energy Systems. 106. 96-104. 10.1016/j.ijepes.2018.09.020.

[15] P. System Relaying Committee of the IEEE Power and E. Society, "IEEE Standard for Synchrophasor Measurements for Power Systems Sponsored by the Power System Relaying Committee IEEE Power & Energy Society," 2011.

[16] I. Power, E. Society, and P. System Relaying, INTERNATIONAL STANDARD Measuring relays and protection equipment-Part 118-1: Synchrophasor for power systems-Measurements. 2018.

[17] M. S. Turiman, M. K. N. M. Sarmin, N. Saadun, L. C. Chong, H. Ali, and Q. Mohammad, "Analysis of High Penetration Level of Distributed Generation at Medium Voltage Levels of Distribution Networks," in 2022 IEEE International Conference on Power Systems Technology: Embracing Advanced Technology in Power and Energy Systems for Sustainable Development, POWERCON 2022, Institute of Electrical and Electronics Engineers Inc., 2022. doi: 10.1109/POWERCON53406.2022.9929780.

[18] A. Harb, W. A. Saliek, and M. Alhusseini, "On the Impacts of Renewable Energy on Distribution Power Systems and the Effects of Energy Storage Systems," in 2023 14th International Renewable Energy Congress, IREC 2023, Institute of Electrical and Electronics Engineers Inc., 2023. doi: 10.1109/IREC59750.2023.10389307.

[19] J. O. Petinrin and M. Shaabanb, "Impact of renewable generation on voltage control in distribution systems," Renewable and Sustainable Energy Reviews, vol. 65, pp. 770–783, Nov. 2016, doi: 10.1016/J.RSER.2016.06.073.

[20] K. Kaushal, P. Syal, and S. K. Sinha, "A Brief Study on Optimal Placement of Phasor Measurement Unit," in 2018 3rd International Innovative Applications of Computational Intelligence on Power, Energy and Controls with their Impact on Humanity (CIPECH), 2018, pp. 215–220. doi: 10.1109/CIPECH.2018.8724316.